J. Phys. Chem. Solids Vol. 40, pp. 797–802
Pergamon Press Ltd., 1979. Printed in Great Britain

^{11}B NUCLEAR QUADRUPOLE INTERACTION IN METAL HEXABORIDES (MB_6)

M. AONO and S. KAWAI
National Institute for Research in Inorganic Materials, Namiki 1-1, Sakura-mura, Niihari-gun, Ibaraki 300-31, Japan

(*Received* 22 *September* 1978; *accepted* 1 *March* 1979)

Abstract—The magnitude of the electric field gradient at the boron nucleus, $|eq|$, in divalent- and trivalent-metal hexaborides (MB_6) as well as in mixed-valent SmB_6 has been measured by the nuclear magnetic resonance method. In each group of divalent- and trivalent-metal hexaborides, $|eq|$ decreases remarkably with increasing lattice parameter. At a given lattice parameter, $|eq|$ for the trivalent-metal hexaborides is smaller than that for the divalent-metal hexaborides. The value of $|eq|$ for SmB_6 is situated between those for the divalent- and trivalent-metal hexaborides. On the basis of these results, the electronic structure of the hexaborides is discussed.

1. INTRODUCTION

Rare-earth and alkaline-earth metals form isomorphous hexaborides (MB_6) which have the crystal structure shown in Fig. 1; the structure consists of a three-dimensional boron framework and metal ions embedded into the interstices. Recently, considerable attention has been paid to a variety of interesting properties of the hexaborides. For example, LaB_6 has an unusually low work function and is expected to be the most promising electron-beam source of high brightness[1–5]. SmB_6 is a remarkable compound in that it contains both Sm^{3+} and Sm^{2+} ions in the ratio of $\sim 7:3$ and exhibits complicated electrical properties[6–11]. Up to this time, a number of experimental and theoretical investigations have been made concerning the electronic structure of the hexaborides[12–18]. It is generally agreed that the boron framework absorbs *two* electrons from each metal atom so as to complete its covalent bonding. Thus, divalent-metal hexaborides are semiconductors while trivalent-metal hexaborides are metals which have one conduction electron per metal ion. In the present study, the magnitude of the nuclear electric quadrupole interaction of ^{11}B in divalent- and trivalent-metal hexaborides as well as in mixed-valent SmB_6 has been measured by NMR (nuclear magnetic resonance). A similar investigation was already made by Gossard and Jaccarino[19], but no experiment was made on divalent-metal hexaborides. The purpose of this paper is to discuss the bonding nature of the hexaborides on the basis of the experimental results on the ^{11}B nuclear electric quadrupole interaction.

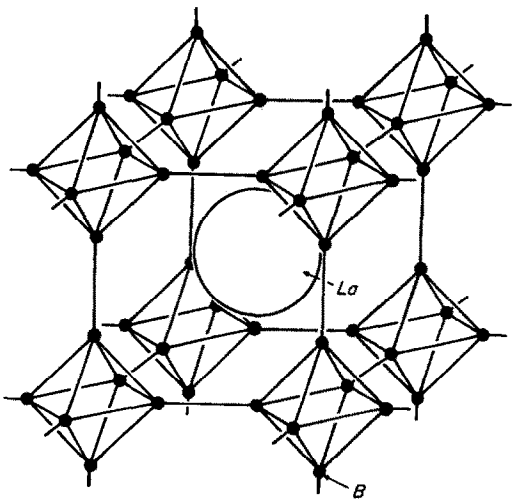

Fig. 1. The crystal structure of metal hexaborides. The structure consists of a boron framework and metal ions embedded into the interstices. The boron framework can be regarded as a simple cubic lattice formed by boron octahedra.

2. EXPERIMENTAL

Rare-earth hexaborides LaB_6, SmB_6, EuB_6, and YbB_6, as well as an alkaline-earth hexaboride CaB_6, have been studied. The rare-earth hexaborides were synthesized by the reaction $2M_2O_3 + 30B = 4MB_6 + 6BO\uparrow$, where M denotes a rare-earth metal, while CaB_6 was synthesized by the reaction $2CaO + 14B = 2CaB_6 + 2BO\uparrow$. In every case, a mixture of the starting materials was placed in a ZrB_2 crucible and heated at $\sim 1700°C$ for about one hour under an argon atmosphere. X-Ray diffraction patterns showed that each reaction product was a single-phase hexaboride.

NMR spectra were measured at room temperature with a wide-line spectrometer at a fixed frequency of 14.50 MHz. The derivative of the adsorption was recorded with a field-modulation lock-in detection method; the field modulation was usually 140 Hz. The external magnetic field was calibrated with the proton resonance.

3. RESULTS

As typical examples, the ^{11}B NMR spectra of LaB_6 and SmB_6 are shown in Fig. 2. The central line is due to the nuclear magnetic Zeeman interaction, and the satellite lines are caused by the nuclear electric quadrupole interaction. Similar spectra were obtained for EuB_6, YbB_6, and CaB_6, although the central lines for EuB_6 were broad and asymmetric because of the internal magnetic field due to magnetic europium ions.

The nuclear electric quadrupole interaction considered

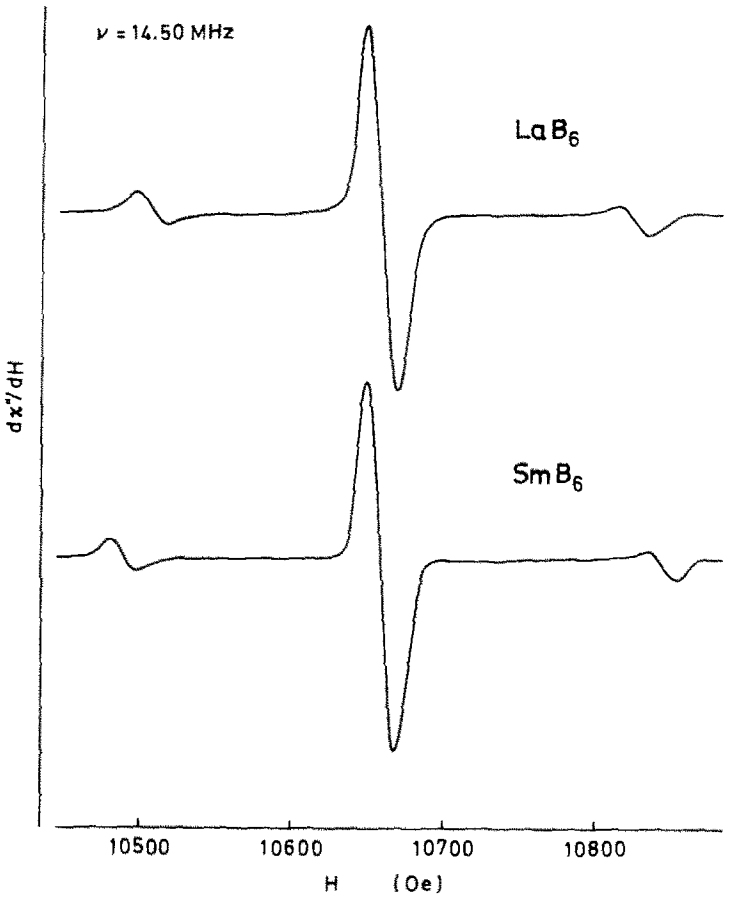

Fig. 2. The ^{11}B NMR spectra of LaB_6 and SmB_6 at room temperature. The NMR frequency is 14.50 MHz, and the field modulation is 140 Hz.

in the present paper is described by the Hamiltonian

$$\hat{H}_Q = \frac{eQ}{4I(2I-1)}[V_{zz}(3\hat{I}_z^2 - \hat{I}^2) + (V_{xx} - V_{yy})(\hat{I}_x^2 - \hat{I}_y^2)], \quad (1)$$

where eQ is the nuclear electric quadrupole moment, I the nuclear spin, $\hat{I}_x$, $\hat{I}_y$, $\hat{I}_z$, and $\hat{I}^2$ the nuclear spin operators, and V_{xx}, V_{yy}, and V_{zz} the principal values of the electric field gradient tensor due to electric charges surrounding the nucleus. In the case of ^{11}B, I is equal to 3/2. As we see in Fig. 1, all the boron sites in the hexaboride structure are crystallographically equivalent and have four-fold symmetry. Therefore, if we chose the local z axis as the symmetry axis, V_{xx} and V_{yy} are equal, and hence the last term in the brackets in eqn (1) vanishes. That is, the nuclear electric quadrupole interaction of ^{11}B in hexaborides is described only by V_{zz}, which customarily denoted by $|eq|$ and is merely called electric field gradient. In the experimental conditions used, the nuclear electric quadrupole interaction of ^{11}B can be treated as a first-order perturbation to the ^{11}B nuclear magnetic Zeeman interaction, and hence we can estimate the magnitude of the coupling constant of the ^{11}B nuclear electric quadrupole interaction, $|e^2qQ|$, from the separation of the satellite lines in the NMR spectra such as those in Fig. 2[20].

The values of $|e^2qQ|$ for various hexaborides estimated in this way, as well as those reported by Gossard and Jaccarino[19], are plotted in Fig. 3 against the lattice parameter a. Since Q for ^{11}B is known as 0.03×10^{-24} cm^2[21], we can convert $|e^2qQ|$ into the magnitude of the electric field gradient, $|eq|$, as indicated on the right hand side of Fig. 3, although $|eq|$ thus estimated is only approximate since the value of Q used is not accurate.

4. DISCUSSION

From the experimental results summarized in Fig. 3, the hexaborides can be divided into three groups. The first group involves EuB_6, YbB_6, and VaB_6, the second group contains SmB_6 only, and the third group consists of the other hexaborides. The hexaborides in the first and third groups are divalent and trivalent, respectively, and SmB_6 of the second group is a mixed-valent compound in which Sm^{2+} and Sm^{3+} ions coexist.

In Fig. 3, the following features are observed: (1) In each group of the divalent- and trivalent-metal hexaborides, the electric field gradient at the boron nucleus, $|eq|$, decreases remarkably with increasing lattice parameter. (2) At a given lattice parameter, $|eq|$ for the trivalent-metal hexaborides is distinctly smaller than that for the divalent-metal hexaborides. (3) The value of $|eq|$ for SmB_6 lies between those for the divalent- and trivalent-metal hexaborides.

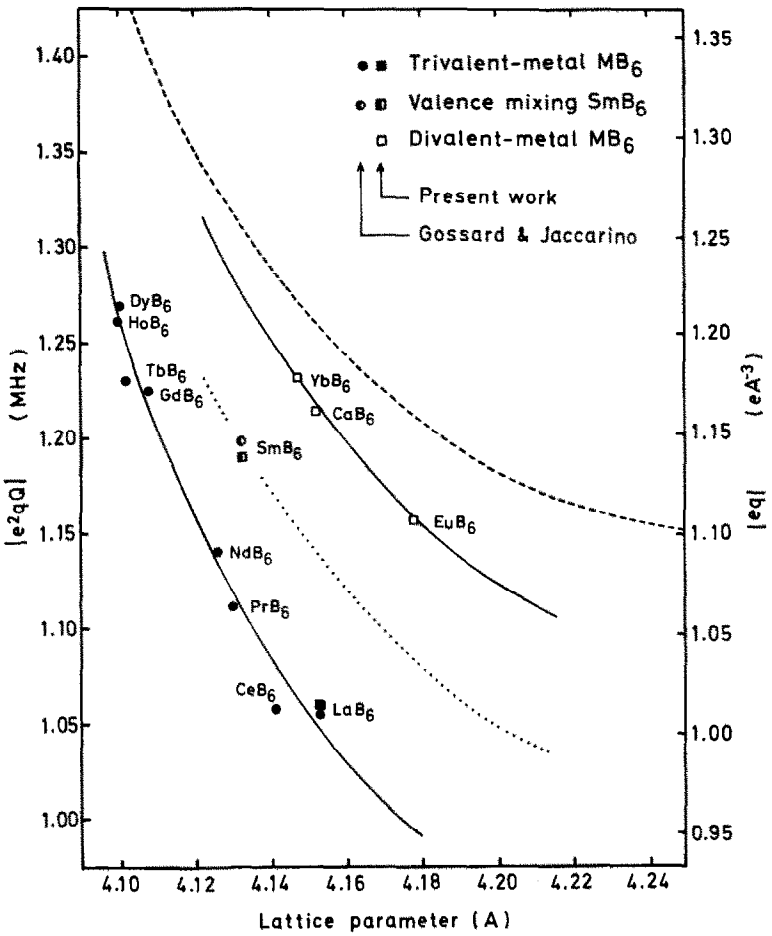

Fig. 3. The magnitude of the ^{11}B nuclear electric quadrupole interaction, $|e^2qQ|$, in divalent- and trivalent-metal hexaborides as well as mixed-valent SmB_6 is plotted against the lattice parameter. The scale on the right-hand side, $|eq|$, shows the magnitude of the electric field gradient at the boron nucleus converted from $|e^2qQ|$. The broken and dotted curves, which should be compared with the experimental curves for the divalent- and trivalent-metal hexaborides, respectively, show the results of theoretical calculations described in the text.

Since the divalent-metal hexaborides have no metallic conduction electrons, their electronic structure is simple compared with that of the trivalent-metal hexaborides, so let us first consider the divalent-metal hexaborides and the origin of the experimental results (1). In early work by Longuet-Higgins and Roberts[12], they carried out a LCAO energy band calculation of the boron framework by neglecting the interaction between boron and constituent metals and tried to explain the electrical properties of the hexaborides on the basis of the calculation. In what follows, let us examine whether this approximation is consistent with the above-mentioned experimental fact (1), that $|eq|$ decreases remarkably with increasing lattice parameter.

For this purpose, we shall calculate the electronic structure of the boron framework as a function of the lattice parameter by neglecting the boron-metal interaction and evaluate $|eq|$ as a function of the lattice parameter on the basis of the calculation. In the evaluation of $|eq|$, constituent divalent-metal ions will be regarded as point charges of $+2e$; this is a necessary consequence of the disregard of the boron-metal interaction. As we see in Fig. 1, the boron framework is a simple cubic lattice formed by boron octahedra. It is known that the intraoctahedral B–B distance is always 1.76 A for all the hexaborides[22]. That is, the size of the boron octahedra is invariant, and only the interoctahedral B–B distance varies for individual hexaborides with different lattice parameters. The electronic structure of the boron framework with a certain lattice parameter can be calculated by allowing the boron octahedra to interact with each other at a spacing determined by the lattice parameter. At first, LCAO-MO's and energy levels of a single boron octahedron were calculated in the Hückel approximation by taking $2s$, $2p_x$, $2p_y$, and $2p_z$ of boron as AO's; the AO's were expressed by Slater functions. The LCAO-MO's thus calculated, which are 24 in number and are classified into 10 irreducible representations of point group O_h, were essentially the same as those obtained by Longuet-Higgins and Roberts[12] despite the fact that they used rougher approximations. The LCAO-MO's calculated in this way will be denoted by ψ^γ ($\gamma = 1, 2, \ldots, 24$). One-electron wave functions of the boron framework can be expres-

sed by the following Block functions:

$$\Psi_{\mathbf{k}}^{\gamma}(\mathbf{r}) = N_{\mathbf{k}}^{\gamma} \sum_{n} \exp(i\mathbf{k}\cdot\mathbf{R}_n)\psi^{\gamma}(\mathbf{r}-\mathbf{R}_n), \qquad (2)$$

where $\mathbf{R}_n = (X_n, Y_n, Z_n)$ is the position of the nth boron octahedron, $\mathbf{k}$ the wave vector, and $N_{\mathbf{k}}^{\gamma}$ the normalization factor estimated by taking overlap integrals between only adjacent boron octahedra into account.

An electron defined by $\Psi_{\mathbf{k}}^{\gamma}(\mathbf{r})$ produces an electric field gradient

$$eq^{e}(\gamma, \mathbf{k}) = -e \int |\Psi_{\mathbf{k}}^{\gamma}(\mathbf{r})|^2 V_{zz}(\mathbf{r})\, \mathrm{d}^3 r \qquad (3)$$

at the boron nucleus chosen as the origin. In eqn (3), $V_{zz}(\mathbf{r})$ denotes the electric field gradient due to a unit charge at $\mathbf{r} = (x, y, z)$:

$$V_{zz}(\mathbf{r}) = \partial^2(1/\mathbf{r})/\partial z^2 = (3z^2 - r^2)/r^5. \qquad (4)$$

Substituting eqn (2) for $\Psi_{\mathbf{k}}^{\gamma}(\mathbf{r})$ in eqn (3) yields

$$eq^{e}(\gamma, \mathbf{k}) = -e(N_{\mathbf{k}}^{\gamma})^2 \sum_{n,m} \exp\{i\mathbf{k}(\mathbf{R}_m - \mathbf{R}_n)\} G(\gamma; n, m) \qquad (5)$$

where

$$G(\gamma; n, m) = \int \psi^{\gamma}(\mathbf{r}-\mathbf{R}_n)\psi^{\gamma}(\mathbf{r}-\mathbf{R}_m) V_{zz}(\mathbf{r})\, \mathrm{d}^3 r. \qquad (6)$$

Most of the integrals $G(\gamma; n, m)$ can be simplified or neglected. Of the intraoctahedral integrals $G(\gamma; n, n)$, those which relate to the central and nearest-neighbor boron octahedra were calculated straightforwardly, where the central boron octahedron is the boron octahedron which contains the boron atom at the origin. As for the other (more distant) boron octahedra, $G(\gamma; n, n)$ were approximated as

$$G(\gamma; n, n) = V_{zz}(\mathbf{R}_n) = (3Z_n^2 - R_n^2)/R_n^5 \qquad (7)$$

since each distant boron octahedron can be regarded as a point. Similarly, as to the interoctahedral integrals $G(\gamma; n, m)$ $(n \neq m)$, they were calculated straightforwardly only when the boron octahedron was one of the central or nearest-neighbor boron octahedra, the others being neglected because of their small values. This approximation, however, results in an underestimation of the total number of electrons, so that in the terms in which the approximation described by eqn (7) is used, $(N_{\mathbf{k}}^{\gamma})^2$ was substituted by $1/N$, N being the total number of boron octahedra. If the positions of the central and nearest-neighbor boron octahedra are denoted by $\mathbf{R}_1$ and $\mathbf{R}_2, \mathbf{R}_3, \ldots$, and $\mathbf{R}_7$, respectively, the above-mentioned approximations allow us to rewrite eqn (5) as follows:

$$eq^{e}(\gamma, \mathbf{k}) = -e(N_{\mathbf{k}}^{\gamma})^2 \Big[\sum_{n=1}^{7} G(\gamma; n, n) + \sum_{m=2}^{7} \exp\{i\mathbf{k}(\mathbf{R}_m - \mathbf{R}_1)\} G(\gamma; 1, m) + \sum_{n=2}^{7} \exp\{i\mathbf{k}(\mathbf{R}_1 - \mathbf{R}_n)\} G(\gamma; n, 1) \Big] - eN^{-1} \sum_{n=8}^{N} (3Z_n^2 - R_n^2)/R_n^5. \qquad (8)$$

The total contribution from all the valence electrons of the boron framework is evaluated by summing up eqn (8) for occupied LCAO-MO's and for allowed $\mathbf{k}$'s in the first Brillouin zone. Since the boron framework has 20 valence electrons per unit cell (18 from six boron atoms and 2 from a constituent metal atom), each of the low-lying 10 LCAO-MO's is occupied by two electrons. Thus, we obtain

$$eq^{e} = -2e \frac{Na^3}{8\pi^3} \sum_{\gamma=1}^{10} \int (N_{\mathbf{k}}^{\gamma})^2 \Big[\sum_{n=1}^{7} G(\gamma; n, n) + \sum_{m=2}^{7} \exp\{i\mathbf{k}(\mathbf{R}_m - \mathbf{R}_1)\} G(\gamma; 1, m) + \sum_{n=2}^{7} \exp\{i\mathbf{k}(\mathbf{R}_1 - \mathbf{R}_n)\} G(\gamma; n, 1) \Big] \mathrm{d}^3 k - 20e \sum_{n=8}^{N} (3Z_n^2 - R_n^2)/R_n^5. \qquad (9)$$

In addition to $|eq|^{e}$ given by eqn (9), there is another contribution from boron cores and divalent metal ions. The boron core consists of a nucleus of $+5e$ plus two 1 s electrons and may be regarded as a point charge of $+3e$ to good approximation. Each divalent metal ion can also be regarded as a point charge of $+2e$ as mentioned before. The distribution of boron cores in the central and nearest-neighbor boron octahedra was correctly considered, but six boron cores of each distant boron octahedron were regarded as a point charge of $+18e$ as a whole. The contribution from these positive charges is thus written as

$$eq^{p} = 3e \sum_{n=1}^{7} {\sum_{j=1}^{6}}' (3Z_{nj}^2 - R_{nj}^2)/R_{nj}^5 + 18e \sum_{n=8}^{N} (3Z_n^2 - R_n^2)/R_n^5 + 2e \sum_{n=1}^{N} (3Z_n'^2 - R_n'^2)/R_n'^5. \qquad (10)$$

The first term in the right-hand side is the contribution from the boron cores of the central and nearest-neighbor boron octahedra, the second term is derived from boron cores of distant boron octahedra, and the third term is due to the divalent metal ions; R_{nj} and Z_{nj} are the radial and z coordinates of the jth boron atom of the nth boron octahedron, respectively, and R_n' and Z_n' are the radial and z coordinates of the nth divalent metal ion, respectively.

The electric field gradient $eq^{e} + eq^{p}$ discussed above distorts the distribution of the 1 s electrons of the boron atom at the origin from spherical symmetry. As a result of this so-called antishielding effect, an additional electric field gradient Δeq is induced. It is necessary to divide Δeq into two parts. One is induced by the electric field

gradient due to the valence electrons of the boron atom at the origin itself, and the other is induced by the remaining electric field gradient due to distant sources. Proportionality constants which are related to the former and the latter are denoted by R and γ_∞, respectively, and, in general, R and γ_∞ are different from each other. In the case of boron, however, R and γ_∞ have close values with the same sign ($R = 0.143$ [23], $\gamma_\infty = 0.145$ [24]), so that we can use a common proportionality constant $\gamma = 0.144$, the average of R and γ_∞.

The electric field gradient at the boron nucleus in the divalent-metal hexaborides is given by

$$eq[M^{2+}(B_6)^{2-}] = (1-\gamma)(eq^e + eq^p), \qquad (11)$$

which is a function of the lattice parameter. The right-hand side of eqn (11) involves three infinite series ($N \to \infty$). These diverge individually but converge as a whole; the evaluation was made by Evjen's method. The value of $eq[M^{2+}(B_6)^{2-}]$ was calculated for three different lattice parameters, $a = 4.11$, 4.18 and 4.25 A, and the results are summarized in the last row of Table 1. The other rows indicate various contributions to $eq[M^{2+}(B_6)^{2-}]$. The broken curve in Fig. 3 shows $eq[M^{2+}(B_6)^{2-}]$ as a function of the lattice parameter. Although quantitative agreement between this curve and the experimental curve for the divalent-metal hexaborides is not complete, the qualitative tendency that experimental $eq[M^{2+}(B_6)^{2-}]$ decreases remarkably with increasing lattice parameter is explained by this calculation. That is, as far as the electric field gradient at the boron nucleus and its change with the lattice parameter are considered, our approximation that the metal-boron interaction in the divalent-metal hexaborides is weak seems to be fairly good.

Next, let us consider the experimental fact (2) mentioned before, that $|eq|$ for the trivalent-metal hexaborides is smaller than that for the divalent-metal hexaborides at a given lattice parameter. The trivalent-metal hexaborides can be obtained by substituting each divalent metal ion in the divalent-metal hexaborides by a trivalent metal ion plus one conduction electron: $M^{2+} \to M^{3+} + e^-$ (conduction electron). If the conduction electrons are uniformly distributed, they make no contribution to the electric field gradient. In this case, it is easy to calculate the difference in $|eq|$ between the divalent- and trivalent-metal hexaborides; the difference is a function of the lattice parameter: $\delta(a)$. In Fig. 3, the dotted curve, which should be compared with the experimental curve for the trivalent-metal hexaborides, has been obtained from the calculation of $\delta(a)$ and the experimental curve for the divalent-metal hexaborides. As we see, this dotted curve is certainly situated below the experimental curve for the divalent-metal hexaborides, but its deviation from the experimental curve for the trivalent-metal hexaborides is large. This indicates that the distribution of conduction electrons in the trivalent-metal hexaborides deviates considerably from a uniform distribution. This is consistent with recent energy band calculations [16, 18] and Fermi surface studies [16, 17] on LaB_6.

The experimental fact (3) mentioned before, that $|eq|$ for SmB_6 lies between those for the divalent- and trivalent-metal hexaborides is easily explained by the

Table 1. The electric field gradient at the boron nucleus in divalent-metal hexaborides, $eq[M^{2+}(B_6)^{2-}]$, calculated as a function of the lattice parameter by neglecting the interaction between boron and constituent metals. Various contributions to $eq[M^{2+}(B_6)^{2-}]$ are also shown

	Electric field gradient at the boron nucleus (eA^{-3})					
	a = 4.11 A		a = 4.18 A		a = 4.25 A	
Boron octahedra at $R_1, R_2, \ldots, R_7$	1.707		1.489		1.412	
Nearest-neighbor eight M^{2+} ions	-0.164	1.543	-0.152	1.337	-0.140	1.272
Other boron octahedra and M^{2+} ions		0.020		0.018		0.015
Total		1.563		1.355		1.287
Correction of shielding effect		-0.225		-0.195		-0.185
$eq[M^{2+}(B_6)^{2-}]$		1.338		1.160		1.102

fact that SmB_6 contains both Sm^{3+} and Sm^{2+} ions in a ratio of $\sim 7:3$ as mentioned in Section 1.

5. SUMMARY

The magnitude of the electric field gradient at the boron nucleus in hexaborides, $|eq|$, decreases remarkably with increasing lattice parameter in each group of divalent- and trivalent-metal hexaborides. This remarkable decrease in $|eq|$ can be explained by a change in the electronic structure of the boron framework due to the increase in the lattice parameter. At a given lattice parameter, $|eq|$ for the trivalent-metal hexaborides is smaller than that for the divalent-metal hexaborides. Analysis of this difference leads us to a conclusion that the distribution of conduction electrons in the trivalent-metal hexaborides deviates considerably from a uniform distribution. The value of $|eq|$ for SmB_6 is situated between those for divalent- and trivalent-metal hexaborides since SmB_6 is a mixed-valent compound which contains both Sm^{2+} and Sm^{3+} ions.

Acknowledgements—We would like to thank Dr. K. Umehara and Dr. T. Chiba for helpful discussions.

REFERENCES

1. Lafferty J. M., *J. Appl. Phys.* **22**, 299 (1951).
2. Broers A. N., *J. Appl. Phys.* **38**, 1991 (1967); **38**, 3040 (1967); *J. Phys. E* **2**, 273 (1969); *Rev. Sci. Instrum.* **40**, 1040 (1969).
3. Vogel S. F., *Rev. Sci. Instrum.* **41**, 585 (1970).
4. Shimizu R., Kataoka Y., Kawai S. and Tanaka T., *Appl. Phys. Lett.* **27**, 113 (1975); *Jap. J. Appl. Phys.* **14**, 1089 (1975).
5. Verhoven J. D. and Gibson E. D., *J. Phys. E* **9**, 65 (1976).
6. Vainshtein E. E., Blokhin S. M. and Paderno Yu. B., *Soviet Phys.—Solid State* **6**, 2318 (1965).
7. Menth A., Buehler E. and Geballe T. H., *Phys. Rev. Lett.* **22**, 295 (1969).
8. Cohen R. L., Eibschütz M., West K. W. and Buehler E., *J. Appl. Phys.* **41**, 898 (1970).
9. Nickerson J. C., White R. M., Lee K. N., Bachmann R., Geballe T. H. and Hull G. W., Jr., *Phys. Rev.* **B3**, 2030 (1971).
10. Aono M., Kawai S., Kono S., Okusawa M., Sagawa T. and Takehana Y., *Solid State Commun.* **16**, 13 (1974).
11. Chazalviel J.-N., Campagna M., Wertheim G. K. and Schmidt P. H., *Phys. Rev.* **B14**, 4586 (1976).
12. Longuet-Higgins H. C. and Roberts M. de V., *Proc. Roy. Soc.* **224**, 336 (1954).
13. Yamazaki M., *J. Phys. Soc. Japan* **12**, 1 (1957).
14. Lipscomb W. N. and Britton D., *J. Chem. Phys.* **33**, 275 (1960).
15. Johnson R. W. and Daane A. H., *J. Chem. Phys.* **38**, 425 (1963).
16. Arko A. J., Crabtree G., Karim D., Mueller F. M., Windmiller L. R., Ketterson J. B. and Fisk Z., *Phys. Rev.* **B13**, 5240 (1976).
17. Ishizawa Y., Tanaka T., Bannai E. and Kawai S., *J. Phys. Soc. Japan* **42**, 112 (1977).
18. Hasegawa A. and Yanase A., *J. Phys. F: Metal Phys.* **7**, 1245 (1977).
19. Gossard A. C. and Jaccarino V., *Proc. Phys. Soc.* **80**, 877 (1962).
20. Slichter C. P., *Principles of Magnetic Resonance.* Harper & Row, New York (1963).
21. Ramsey N. F., *Nuclear Moments.* Wiley, New York (1953).
22. Kunnmann W., *Preparation and Properties of Solid State Materials* (Edited by R. A. Lefever). Marcel Dekker, New York (1971).
23. Sternheimer R. M., *Phys. Rev.* **105**, 158 (1957).
24. Das T. P. and Bersohn R., *Phys. Rev.* **102**, 733 (1956).